SUPPORTING INFORMATION

A fluorescent, reagentless biosensor for ATP, based on malonyl-coenzymeA synthetase

Renée Vancraenenbroeck and Martin R. Webb

The Francis Crick Institute, Mill Hill Laboratory, The Ridgeway, Mill Hill, London NW7 1AA, UK

Corresponding author: martin.webb@crick.ac.uk

Supporting Method: Generation of Rho-MatB

Plasmids. Plasmid pRpMatB39 (plasmid pTEV5, containing the coding sequence of RpMatB (Genbank accession number CAE25665.1) with the point mutation K488A and an N-terminal His_6-tag) was provided by J.C. Escalante-Semerena (University of Georgia, Athens, GA, USA)[1]. The QuikChange site-directed mutagenesis protocol and the QuikChange Lightning Multi site-directed mutagenesis kit (Stratagene) were used for single-site or multi-site mutations of the pRpMatB39 plasmid, respectively. The primers to introduce the point mutation C106A in the pRpMatB39 plasmid are 5'-ccgaagatcgtggtggccgatccgtccaagcg-3' and 5'-cgcttggacggatcggccaccacgatcttcgg-3'. The primers to introduce R286C and Q457C, i.e. the mutations in the final biosensor, are respectively 5'-gctcgccgatacgcattgcgaatggtcg-3' and 5'-acgatcgacgaagcgtgcgtgctgcacggcctc-3'.

Protein expression and purification. RpMatB variants were expressed in *E. coli* OverExpress C41(DE3) cells (Lucigen). The cell pellet of a 5 ml overnight culture, grown at 37 °C and supplemented with 100 μg ml^{-1} ampicillin, was resuspended in 0.5 l of lysogeny broth, supplemented with ampicillin, in 5 l shaker flasks and cultured via vigorous shaking at 30 °C to an optical density at 600 nm of 0.6 - 0.8 cm^{-1}. Then 0.5 mM isopropyl-β-D-thiogalactoside was added to start induction at 30 °C for 16 h. After induction, the cultures were cooled to 4 °C and centrifuged at 3500 rpm for 30 min at 4 °C (rotor JS 4.2, Beckman). The cell pellet was washed with 30 ml of ice-cold buffer (10 mM Tris.HCl pH 7.5, 300 mM NaCl), centrifuged at 3500 rpm for 30 min at 4 °C, the supernatant discarded and the pellet stored at -80 °C. Typically ~3 g wet weight of *E. coli* cells was harvested from 0.5 l culture.

The cell pellet was resuspended in 35 ml 30 mM Tris.HCl, 300 mM NaCl, 10 mM imidazole, 3 mM tris(2-carboxyethyl)phosphine, 2 mM phenylmethanesulfonyl fluoride, pH 8.0 and sonicated on ice using an ultrasonicator (VC505, Sonics) at 200 W for 5 times 30 s with a 5 s on / 5 s off pulse. The soluble fraction was collected by centrifugation at 35000 rpm for 45 min at 4 °C (rotor 45 Ti, Beckman). The His_6-tagged protein was purified at 4 °C by immobilized metal ion affinity chromatography (1 ml HisTrap HP column, GE Healthcare) using an Äkta system (GE Healthcare). The resin was equilibrated with Buffer A (30 mM Tris.HCl, 300 mM NaCl, 10 mM imidazole, 1 mM tris(2-carboxyethyl)phosphine, pH 8.0). The sample was filtered (0.45 μm Minisart NML filter, Sartorius) and loaded onto the column at 0.5 ml min^{-1}. The column was washed with 20 ml Buffer A and additionally with 20 ml of 95% Buffer A and 5% Buffer B (30 mM Tris.HCl, 300 mM NaCl, 250 mM imidazole, 1 mM tris(2-carboxyethyl)phosphine, pH 8.0) at a flow rate of 1 ml min^{-1}. The protein was eluted with 20 ml of Buffer B at a flow rate of 1 ml min^{-1}. Protein fractions were pooled (~2-4 ml) and further purified via size exclusion chromatography at 4 °C using the HiLoad 16/60 Superdex 200 prep grade column (GE Healthcare) equilibrated with 30 mM Tris.HCl, 100 mM NaCl, 0.5 mM ethylenediaminetetraacetic acid, 5 mM dithiothreitol, 1 mM NaN_3 at 1 ml min^{-1}.

Fractions containing the protein were pooled and concentrated (VivaSpin 20 MWCO 10 kDa cut off, GE Healthcare) to ~10 mg ml^{-1}. The protein concentration was determined from the absorbance at 280 nm using the extinction coefficient at 280 nm of 46300 M^{-1} cm^{-1} calculated from the sequence via Expasy Protparam[2]. The protein was drop-frozen in liquid nitrogen and stored at -80 °C. Typically, 45 mg of protein was obtained from 3 g wet weight of cells.

Labeling MatB. Labeling and purification are described for the final sensor variant RpMatB ((His$_6$/C106A/R286C/Q457C/K488A)RpMatB). Any differences from this procedure for other RpMatB variants are described after.

Dithiothreitol was removed from ~40 mg of RpMatB using a PD10 desalting column (GE Healthcare) pre-equilibrated with Buffer L (30 mM Tris.HCl pH 7.5, 100 mM NaCl) at 20 °C. 50 µM protein was incubated at 20 °C with 225 µM 5-IATR (AnaSpec) in Buffer L using an end-over-end mixer for 90 min. Then 2 mM sodium-2-mercaptoethanesulfonate was added and incubation continued for 15 min. After centrifugation at 3500 rpm for 15 min at 4 °C (Heraeus Biofuge), the supernatant was filtered through a 0.2 µm syringe filter (Acrodisc Syringe Filter with HT Tuffryn Membrane, Pall Life Sciences) and loaded onto a PD10 desalting column, equilibrated with Buffer Q1 (30 mM Tris.HCl pH 8.0, 25 mM NaCl) at ~20 °C to remove free label.

The final biosensor was further purified via ion exchange chromatography at 4 °C using a 1 ml HiTrap Q HP column (GE Healthcare), equilibrated in Buffer Q1 at 1 ml min^{-1}. After sample loading, the column was washed with 90 ml Buffer Q1. The protein was eluted using a gradient from 100% Buffer Q1 to 50% Buffer Q1 and 50% Buffer Q2 (30 mM Tris.HCl pH 8.0, 1 M NaCl) over 25 ml followed by a gradient from 50% Buffer Q1 and 50% Buffer Q2 to 100% Buffer Q2 over 10 ml. Rho-MatB eluted as two overlapping peaks with identical mass and fluorescence properties. Both peaks were pooled and concentrated to ~5 mg ml^{-1} using a concentrator (Amicon Ultra-4 10 kDa cut off, Millipore).

While screening for a fluorescence change upon ATP binding, labeling was performed on a scale of ~2 mg of protein. RpMatB variants (100 µM) were incubated at 20 °C with 2-fold excess MDCC over RpMatB for 35 min, or with 2-fold excess IDCC for 120 min, or with 4-fold excess 5-IATR or 6-IATR for 90 min. During screening, the labeled RpMatB variants were purified only using a PD10 desalting column.

The labeled protein concentrations were determined using the following extinction coefficients: RpMatB: ε_{280} (46300 M^{-1} cm^{-1}), tetramethylrhodamine: ε_{280} (31000 M^{-1} cm^{-1}) and ε_{528} (52000 M^{-1} cm^{-1})[3], MDCC: ε_{280} (7470 M^{-1} cm^{-1}) and ε_{430} (46800 M^{-1} cm^{-1}) and IDCC: ε_{280} (7470 M^{-1} cm^{-1}) and ε_{430} (44800 M^{-1} cm^{-1})[4]. The protein was drop-frozen in liquid nitrogen and stored at -80 °C. Labeling yields were up to 35%.

Using mass spectrometry, unlabeled RpMatB ((His$_6$/C106A/R286C/Q457C/K488A)RpMatB) had a mass of 57335.9 Da. The theoretical molecular weight is 57324.2 Da, assuming loss of the N-terminal methionine. Presumably, other post-translational modifications, such as partial oxidation of surface-accessible methionines, occur[5]. The final biosensor, Rho-MatB ((5-ATR)2-(His$_6$/C106A/R286C/Q457C/K488A)RpMatB), had a mass of 58216.4 Da, conforming to the theoretical molecular weight of the RpMatB protein with two 5-ATRs attached (57335.9 + 2 × 441.5).

Supporting Method: Global fitting of association time courses

The global best-fit values and confidence intervals for rate constants that describe the binding of ATP to RhoMatB, using the conformational selection scheme (Figure 5A). A set of data with ATP in excess and one with protein in excess were fit using KinTek Global Kinetic Explorer (v 4.0)[6, 7]. Data points with $t < 0.002$ s in all data sets were removed as they were within the dead time of the stopped flow instrument. An initial incubation step was included in the calculations to enable the two apo conformations, Rho-$MatB_1$ and Rho-$MatB_2$, to equilibrate before addition of ATP.

The fluorescence change in the fitting was described by a differential fluorescence factor, which was the difference between the fluorescence of apoprotein and ATP-bound Rho-MatB to relate fluorescence to concentration. Experimental traces with excess protein and with excess ATP were from different experimental protocols, requiring different instrumental settings and resulting in different absolute fluorescence values. Therefore, different fluorescence factors were used for the two types of experiments. The starting fluorescence values (offsets) were treated as adjustable model parameters.

A one-dimensional FitSpace calculation[6] was used to determine the range over which each rate constant can vary, while still allowing an acceptably good fit within a Chi^2 threshold of 1.2-fold of the minimum value. The fluorescence enhancement factor was allowed to vary along with rate constants, but offset values were fixed during this calculation.

Table S1: Fluorescence changes for binding of ATP and ADP to fluorophore-RpMatB adducts. Cysteine mutations were introduced into (His_6/C106A/K488A)RpMatB. Diethylaminocoumarin, using MDCC or IDCC, or tetramethylrhodamine, using 5-IATR or 6-IATR, were covalently linked to the protein. Data are from a survey without complete optimization of the labeling and purification. The fluorescence changes (F_+/F_-) upon ligand binding were obtained by excitation at 553 nm and emission at 577 nm for tetramethylrhodamine and excitation at 431 nm and emission at 470 nm for diethylaminocoumarin at 20 °C in 50 mM Tris.HCl pH 7.5, 100 mM NaCl, 10 mM $MgCl_2$, 0.3 mg ml^{-1} bovine serum albumin using 1 μM RpMatB adduct with or without saturating ATP.

Cysteine Mutations	**Labeling reagent**	$\boldsymbol{F_+/F_-}$
N492C	MDCC	0.6
N492C[a]	IDCC	0.4
E496C	MDCC	0.7
V493C	MDCC	0.9
G398C	MDCC	0.9
K399C	MDCC	1.0
D400C	MDCC	0.7
E439C	MDCC	1.6
E388C/Q456C	6-IATR	1.3
E388C/D463C	6-IATR	1.3
R286C/G461C	6-IATR	1.6
K385C/E417C	6-IATR	0.9
K385C/K470C	6-IATR	0.5
S289C/E417C	6-IATR	1.1
R286C/Q457C[b]	6-IATR	2.0
R286C/Q457C	5-IATR	2.9

[a]Values were obtained for the fluorescence ratio with ADP (0.5), the dissociation constant for ATP (0.6 μM) and for ADP (98 μM), as described in the text for Rho-MatB.

[b]Values were obtained for the fluorescence ratio with ADP (1.9), the dissociation constant for ATP (2.7μM) and for ADP (293 μM), as described in the text for Rho-MatB.

Table S2. Comparison between apo and holo (ATP or analogue-bound) structures of ANL superfamily proteins. To investigate the degree of the conformational change after ATP-binding within the ANL superfamily, 5 apo-holo protein pairs[8] (http://labs.hwi.buffalo.edu/gulick/table.html) are shown. In total, 11 holo molecules and 25 apo molecules were analyzed. The C-terminal domain was not present in 11 out of the 25 apo structures. It was either unresolved, hence assumed to be flexible (e.g. PDB 3IVR and PDB 4LGC), or not present in the purified protein (e.g. PDB 3T5B and PDB 3WV4).

The structural relationship between apo and holo structures was determined, based on the root mean square deviation (RMSD) of the α-carbon atoms of aligned residues using SuperPose[9]. The table shows that not only RpMatB but also other ANL superfamily members undergo a conformational change after ATP (or analogue) binding, although in two cases, the apo crystals had multiple structures, including one similar to the closed (ligand-bound) structure, based on the low RMSD.

The relative interdomain orientations were visually inspected for the placement of the C-terminal domain with respect to its N-terminal domain after superposing the N-terminal domains. For the holo molecules, 9 out of 11 structures had conserved interdomain geometry. In contrast, the superposition of the apo molecules showed large variations in the positioning of the C-terminal domain relative to the N-terminal domain.

Protein	**Apo**		**Holo**		**apo - holo**
	PDB ID	**Rcn[a]**	**PDB ID**	**Rcn[a]**	**RMSD (Å)**
Streptococcus pyogenes D-alanine-poly(phosphoribitol) ligase subunit 1	3L8CA[b]	1.4	3LGXA	1.3	0.81
	3L8CB[b]	1.0			3.94
Bacillus cereus D-alanine-poly(phosphoribitol) ligase subunit 1	4PZP[c]	1.1	3FCC	1.1	0.84
Homo sapiens Acyl-coenzyme A synthetase ACSM2A	3B7W	1.4	3C5E	1.5	9.54
RpMatB	4FUQA	1.3	4FUT	1.5	6.18
Thermus thermophilus long-chain-fatty-acid-coenzyme A synthetase	1ULTA[b]	1.7	1V25A	3.4	8.90
	1ULTB[b]	3.1			6.38

[a]Ratio of the average B-factor for the C-terminal domain using all atoms of the C-terminal domain and that of the N-terminal domain.

[b]These crystals contained molecules that had two different conformations. Both conformations were used in the analysis.

[c]Only partially resolved C-terminal domain.

Table S3: Fluorescence of Rho-MatB with various ligands. Fluorescence emission of 1 µM Rho-MatB in 50 mM Hepes pH 7.0, 100 mM NaCl and 0.3 mg ml^{-1} bovine serum albumin, with different ligands present, were measured by excitation at 553 nm and emission at 577 nm. F_+/F_- is the ratio of fluorescence with and without the added ligand.

Buffer addition	**Ligand**	F_+/F_-
10 mM $MgCl_2$	250 µM AMP	1.15
10 mM $MgCl_2$	250 µM GDP	0.97
10 mM $MgCl_2$	250 µM GTP	1.03
10 mM $MgCl_2$	1 mM malonate	0.94
10 mM $MgCl_2$	0.25 mM coenzyme A	0.96
10 mM $MgCl_2$	1 mM malonate and 0.25 mM coenzyme A	0.92
10 mM $MgCl_2$	1 mM malonate, 0.25 mM coenzyme A and 1 mM ATP	3.29
0.5 mM EDTA	250 µM ATP	0.99
0.5 mM EDTA	250 µM ATP and 10 mM $MgCl_2$	3.48

Table S4: Fluorescence changes and dissociation constants for ATP binding to Rho-MatB in different solution conditions. The fluorescence changes upon ATP binding were obtained by excitation at 553 nm and emission at 577 nm at 20 °C in the buffer and salt conditions shown using 1 µM protein and excess ATP in the presence of 10 mM $MgCl_2$ and 0.3 mg ml^{-1} bovine serum albumin. The equilibrium dissociation constants (K_d) were obtained from fluorescence titrations at 20 °C in the buffer mentioned using 0.5 µM protein and various concentrations of ATP. F_+/F_- is the ratio of fluorescence with and without the added ligand.

Buffer	Salt	K_d (µM)	F_+/F_-
50 mM Hepes pH 7.0	100 mM NaCl	6.4 ± 0.6	3.9
50 mM Mes pH 6.0	100 mM NaCl	ND	1.5
50 mM Mes pH 6.5	100 mM NaCl	26 ± 2	2.8
50 mM Hepes pH 7.5	100 mM NaCl	5.6 ± 0.6	3.1
50 mM Tris.HCl pH 7.5[a]	100 mM NaCl	6.0 ± 0.4	2.9
50 mM Hepes pH 8.0	100 mM NaCl	4.6 ± 0.2	3.3
50 mM Bicine pH 8.5	100 mM NaCl	4.4 ± 0.4	3.0
50 mM Bicine pH 9.0	100 mM NaCl	ND	2.6
50 mM Hepes pH 7.0	50 mM NaCl	5.8 ± 0.3	3.4
50 mM Hepes pH 7.0	200 mM NaCl	19 ± 1	3.3

[a]Protein for this measurement was purified only by gel filtration chromatography.

Table S5: Rate constants obtained from global fitting of the conformational selection model to association kinetic data. The model is in Figure 5A and Figure S3 shows the fitted curves. Confidence ranges were obtained for rate constants with Chi^2 being within 1.2-fold that of the best fit value, while allowing other parameters (rate constants and fluorescence factors) to vary: see Supporting Method.

Rate constant	Best-fit value	Standard error	Range
k_{+1}	0.78 s^{-1}	0.02	0.75 - 0.83
k_{-1}	2.0 s^{-1}	0.1	1.9 - 2.10
k_{+2}	2.4 $\mu M^{-1}s^{-1}$	0.2	2.1 - 2.9
k_{-2}	6.9 s^{-1}	0.6	5.9 -8.3

Figure S1: Association and dissociation kinetics of Rho-MatB and ATP. Data were obtained as described in Figure 4. Experimental traces are in black, fitted curves in green. The values of fitted parameters are in Figure 4. (**A**) Rho-MatB at the micromolar concentrations indicated, which were in 10-fold excess over ATP. Data were fit to a single exponential. (**B**) ATP in excess at the micromolar concentrations shown. Data were fit to a single exponential and slope, to obtain the parameters for the fast phase. Note that the dead time of the stopped-flow instrument is ~2 ms, so that the traces only record changes from that time. (**C**) As panel B, but over long times. Data were fit to two exponentials using a fixed rate constant for the fast phase, determined from the short time scale traces in panel B. The rate constant for the slow phase did not vary with concentration and had an average value of 0.88 ± 0.13 s^{-1}.

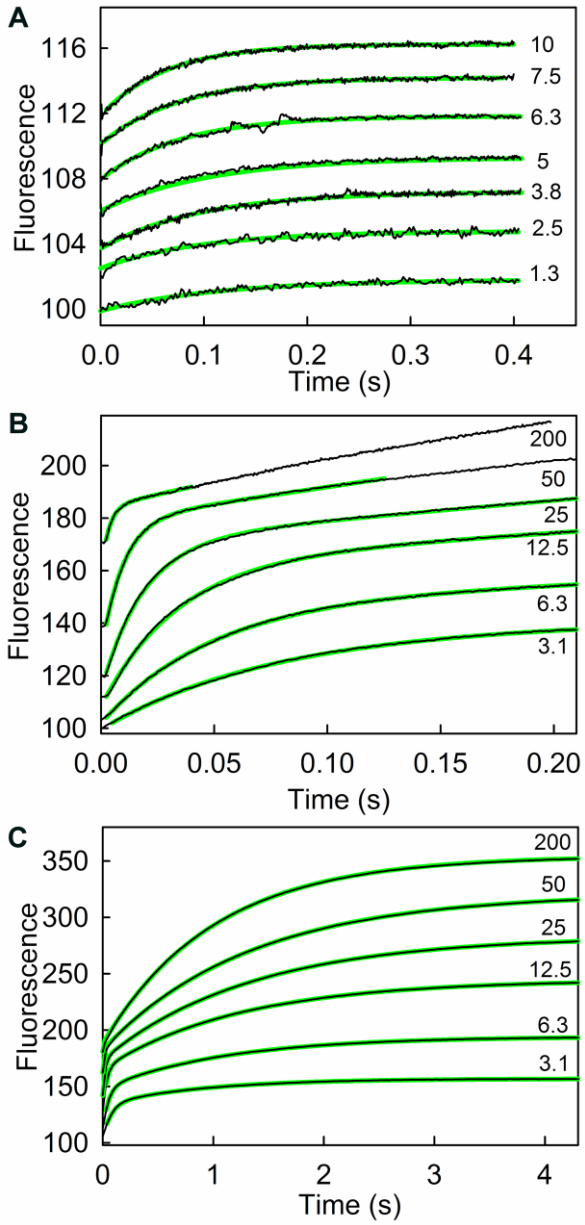

Figure S2: Simulated time courses of ATP binding to Rho-MatB. Simulations used the conformational selection (**A-C**) or induced fit model reaction schemes (**D-F**), shown in Figure 5. Simulations used the same initial concentrations as experiments (Figures 4 and S1) with excess Rho-MatB (**A**, **D**) (traces each offset by 2 for clarity) or excess ATP (**B**, **C**, **E**, **F**). Rate constants included those obtained from exponential fits (Figure S1). The simulated fluorescence signal assumed 3.7-fold difference between apo Rho-MatB and Rho-MatB*·ATP, as that was the enhancement shown experimentally. (**A-C**) For the conformational selection model, it was assumed that initially [Rho-$MatB_1$] = [Rho-$MatB_2$], that is at equilibrium, and these species have the same fluorescence. Rate constants were k_{+1} = 0.88 s^{-1}, k_{-1} = 0.88 s^{-1}, k_{+2} = 1.83 μM^{-1} s^{-1} and k_{-2} = 8.15 s^{-1}. The value of k_{-1} is unknown, but the curve shapes did not critically depend on the value chosen. **(D-F)** Simulations using the induced fit model using rate constants, k_{+1} = 1.83 μM^{-1} s^{-1}, k_{-1} = 8.15 s^{-1}, k_{+2} = 0.88 s^{-1} and k_{-2} = 0 s^{-1}. It also assumed Rho-MatB·ATP has 2-fold higher fluorescence than the apo protein, to give relative amplitudes of the two phases as observed experimentally. For all curves there was no further attempt to obtain amplitudes that exactly matched experimental data. Particularly with excess Rho-MatB, these amplitudes are affected by background levels and optics.

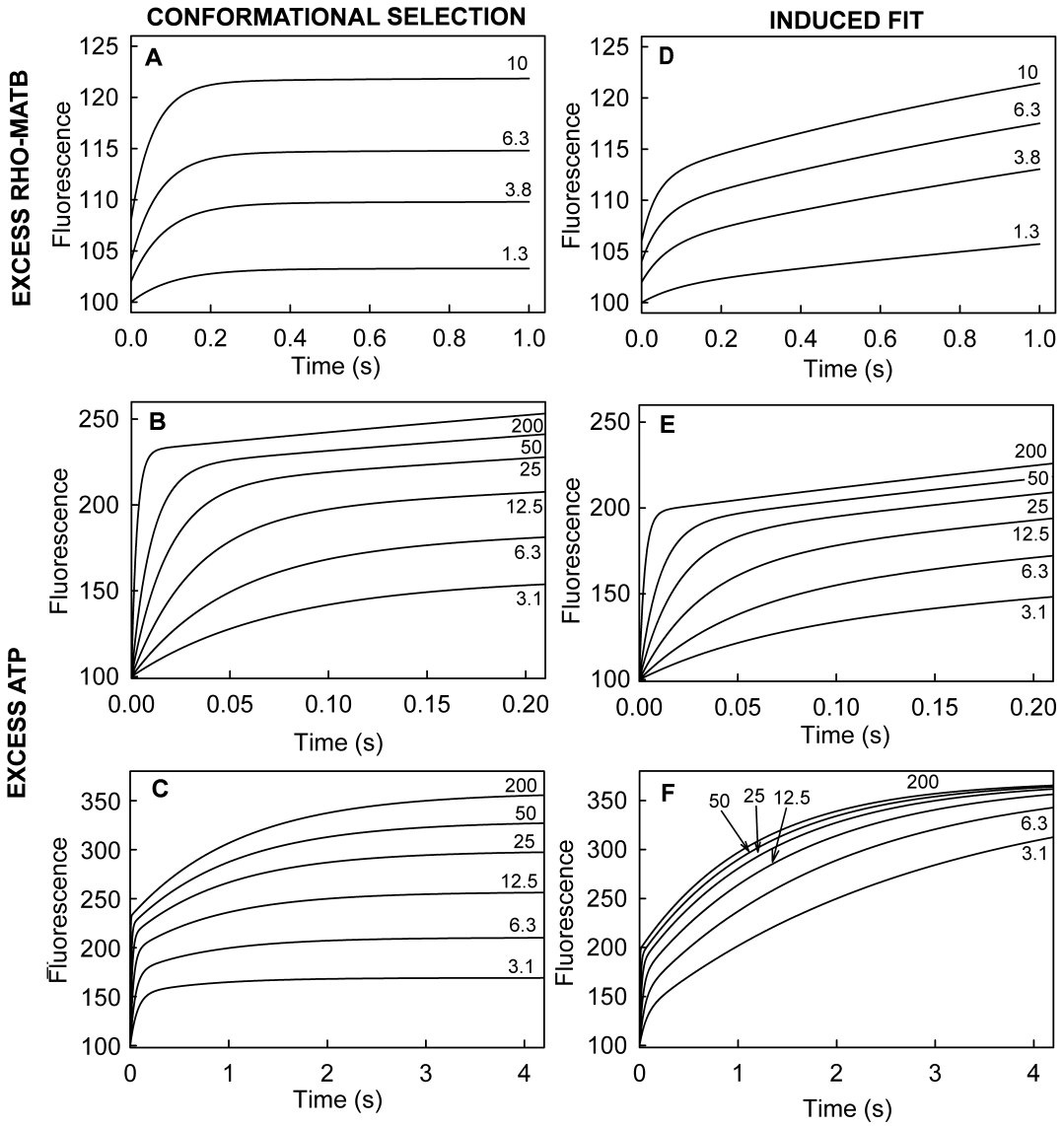

Figure S3: Global fitting of association transient time courses. A complete set of association data (see Figures 4 and S1) with both excess RhoMatB (A) and excess ATP (B, short times, C, long times) were fitted globally to the conformational selection model (Figure 5A). Further information is in the Supporting Method. The fitting procedure included a pre-incubation to enable the two apo conformations, Rho-MatB_1 and Rho-MatB_2, to equilibrate before addition of ATP. Like the simulations in Figure S2, it was assumed that the fluorescence of Rho-MatB_1 equals that of Rho-MatB_2. Note this aspect was not well tested by this fitting, as small difference in the intensities will be reflected only in the relative amplitudes of the two phases. The amplitudes of the rapid phase are not accurate due to their small size (excess Rho-MatB) and loss of signal during the instrument dead time (excess ATP). Experimental traces are solid lines, fitted curves are dashed. The concentrations of the species in excess are shown for each curve. Traces at high [Rho-MatB] were excluded as the high concentrations affected the fluorescence amplitudes due to the inner filter effect. The resulting rate constants and statistics are in Table S5.

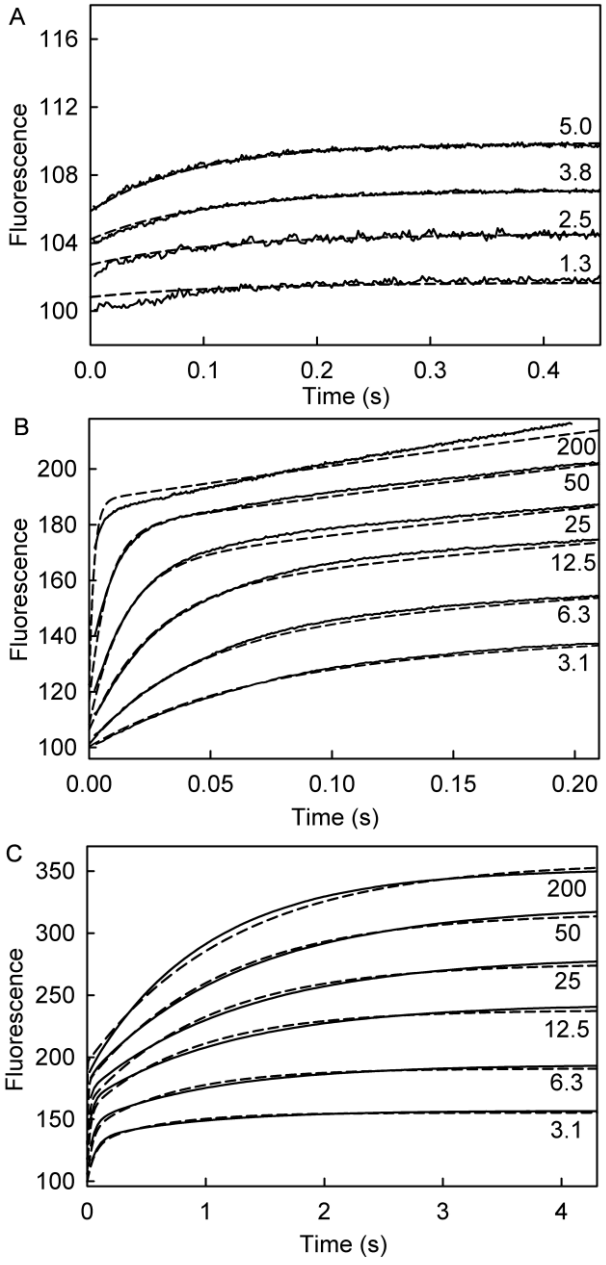

Figure S4: Oligomerization of RpMatB and Rho-MatB, analyzed by SEC-MALLS. The solution molecular weight was analyzed using size exclusion chromatography coupled to multi-angle laser light scattering (SEC-MALLS). Rho-MatB (blue) and (His_6/C106A/R286C/Q457C/K488A)RpMatB (red) were analyzed by SEC-MALLS in the absence (**A**) or presence of MgATP (**B**). The differential refractive index (to show the protein peaks) and the molar mass distributions were plotted against time.

~15 µM Rho-MatB or (His6/C106A/R286C/Q457C/K488A)RpMatB were applied in a volume of 100 µl to a Superdex 200 10/300 GL column (GE Healthcare) connected to a Jasco PU-1580 HPLC at a flow rate of 0.5 ml min^{-1}. The HPLC system was connected to a Dawn Heleos II light scattering instrument (Wyatt Technology) and Optilab T-rex differential refractometer (Wyatt Technology). The solution molecular weight was determined from the combined data from both detectors using the ASTRA software version 6.1.1.17 (Wyatt Technology) with the refractive index increment set to 0.1860 ml g^{-1}. The analysis was at ~20 °C in 30 mM Tris.HCl pH 7.5, 100 mM NaCl, 3 mM NaN_3 with or without MgATP (5 mM $MgCl_2$, 50 µM ATP).

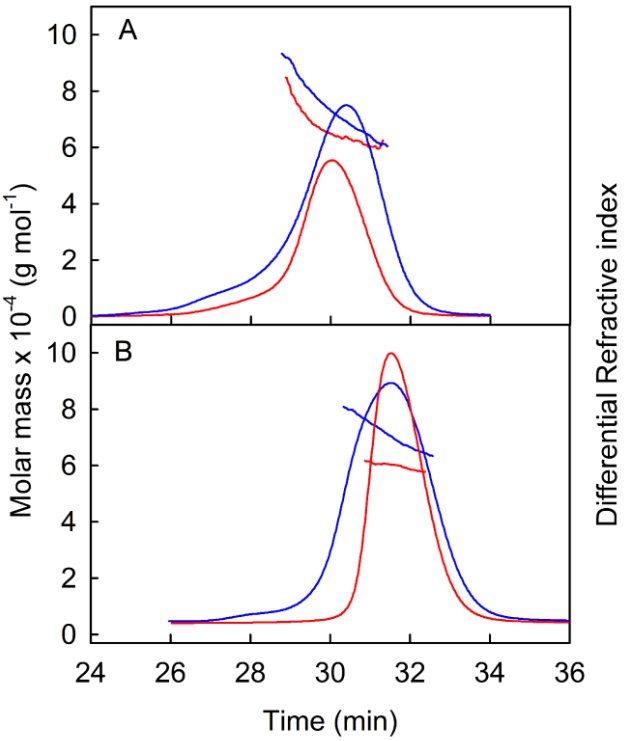

Figure S5: Rho-MatB activity assay. The time course of NADH oxidation in the presence of Rho-MatB was used to determine the residual enzymatic activity of Rho-MatB. Reaction mixtures (200 µl) contained 50 mM Hepes buffer pH 7.5, 25 mM NaCl, 25 mM KCl, 0.3 mg ml^{-1} bovine serum albumin, 0.5 mM ATP, 0.5 mM coenzyme A, 10 mM $MgCl_2$, 3 mM phosphoenolpyruvate, 0.2 mM NADH, 0.01 U $µl^{-1}$ pyruvate kinase, 0.05 U $µl^{-1}$ adenylate kinase, 0.015 U $µl^{-1}$ lactate dehydrogenase and 2 mM malonate. The reaction was started by the addition of 3 µM Rho-MatB and the change in A_{340} was monitored in time at 25 °C. As controls, the activity of 3 µM (His_6/C106A/R286C/Q457C/K488A)RpMatB, that is the unlabeled variant used for the biosensor, or 0.03 µM (His_6/C106A/R286C/Q457C)RpMatB, that is without the K488A mutation, were also measured. Example time courses are shown: the Rho-MatB trace and the control without MatB partially overlay.

The specific activities, as micromolar AMP formed per micromolar MatB were 28 s^{-1} for (His_6/C106A/R286C/Q457C)RpMatB, 34 s^{-1} for Rho-(His_6/C106A/R286C/Q457C)RpMatB (not shown) , but Rho-MatB the activity was $<10^{-3}$ s^{-1}.

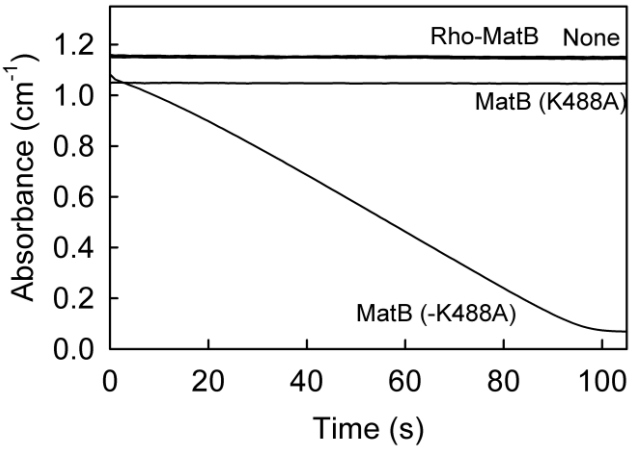

Figure S6: The production of ATP by pyruvate kinase, monitored by a coupled-enzyme assay. (A) Reaction mixtures (200 µl) contained 50 mM Tris.HCl pH 7.5, 100 mM NaCl, 10 mM $MgCl_2$, 100 mM KCl, 0.3 mg ml^{-1} bovine serum albumin, 250 µM ADP, 200 µM NADH, 5 U ml^{-1} lactate dehydrogenase and the micromolar concentrations of phosphoenolpyruvate shown. Reactions were started by the addition of pyruvate kinase (0.10 U ml^{-1}) and the change in A_{340} was monitored at 20 °C using a microplate reader. **(B)** The initial rates (v_i) were determined by linear regression and were plotted versus phosphoenolpyruvate concentration. The parameters K_m (173 ± 19 µM) and V_{max} (0.063 ± 0.002 µM s^{-1}) were obtained by fitting to the Michaelis-Menten model. The average K_m and V_{max} values (n=5) are 251 ± 28 µM and 0.065 ± 0.002 µM s^{-1}, giving a specific activity of 0.65 µM s^{-1} U^{-1} ml.

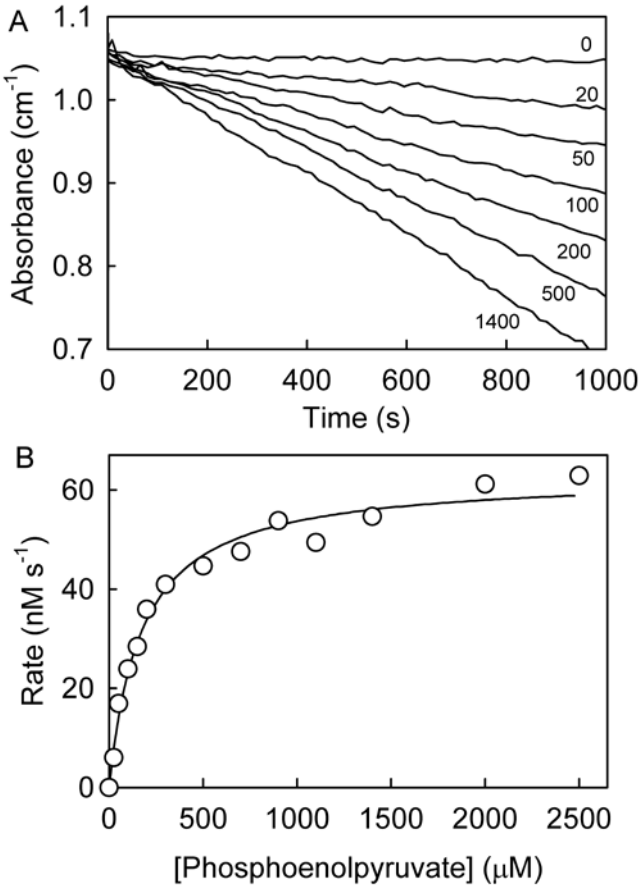

SUPPORTING INFORMATION REFERENCES

1. Crosby, H. A.; Rank, K. C.; Rayment, I.; Escalante-Semerena, J. C., Structure-guided expansion of the substrate range of methylmalonyl coenzyme A synthetase (MatB) of *Rhodopseudomonas palustris*. *Appl. Environ. Microbiol.* **2012,** 78, 6619-6629.
2. Wilkins, M. R.; Gasteiger, E.; Bairoch, A.; Sanchez, J. C.; Williams, K. L.; Appel, R. D.; Hochstrasser, D. F., Protein identification and analysis tools in the ExPASy server. *Methods Mol. Biol.* **1999,** 112, 531-552.
3. Corrie, J. E. T.; Craik, J. S., Synthesis and characterisation of pure isomers of iodoacetamidotetramethylrhodamine. *J. Chem. Soc. Perkin Trans. I* **1994**, 2967-2973.
4. Corrie, J. E. T., Thiol-reactive fluorescent probes for protein labelling. *J. Chem. Soc. Perkin Trans. I* **1994**, 2975-2982.
5. Guan, Z.; Yates, N. A.; Bakhtiar, R., Detection and characterization of methionine oxidation in peptides by collision-induced dissociation and electron capture dissociation. *J. Am. Soc. Mass Spec.* **2003,** 14, 605-613.
6. Johnson, K. A.; Simpson, Z. B.; Blom, T., FitSpace explorer: an algorithm to evaluate multidimensional parameter space in fitting kinetic data. *Anal. Biochem.* **2009,** 387, 30-41.
7. Johnson, K. A.; Simpson, Z. B.; Blom, T., Global Kinetic Explorer: A new computer program for dynamic simulation and fitting of kinetic data. *Anal. Biochem.* **2009,** 387, 20-29.
8. Gulick, A. M., Conformational dynamics in the Acyl-CoA synthetases, adenylation domains of non-ribosomal peptide synthetases, and firefly luciferase. *ACS Chem. Biol.* **2009,** 4, 811-827.
9. Maiti, R.; Van Domselaar, G. H.; Zhang, H.; Wishart, D. S., SuperPose: a simple server for sophisticated structural superposition. *Nucleic Acids Res.* **2004,** 32, W590-594.